Original Article

MOLECULAR METABOLISM

Endocannabinoids regulate cocaine-associated memory through brain AEA–CB1R signalling activation

Hongchun Li [1,*,5], Rong Chen [1,5], Yuanyi Zhou [1], Haichuan Wang [2], Luqiang Sun [3], Zhen Yang [4], Lin Bai [4], Jie Zhang [4]

ABSTRACT

Objective: Contextual drug-associated memory precipitates craving and relapse in substance users, and the risk of relapse is a major challenge in the treatment of substance use disorders. Thus, understanding the neurobiological underpinnings of how this association memory is formed and maintained will inform future advances in the treatment of drug addiction. Brain endocannabinoids (eCBs) signalling has been associated with drug-induced neuroadaptations, but the role of lipases that mediate small lipid ligand biosynthesis and metabolism in regulating drug-associated memory has not been examined. Here, we explored how manipulation of the lipase fatty acid amide hydrolase (FAAH), which is involved in mediating the level of the lipid ligand anandamide (AEA), affects cocaine-associated memory formation.

Methods: We applied behavioural, pharmacological and biochemical methods to detect cocaine-associated memory formation, eCBs in the dorsal dentate gyrus (dDG), and the activity of related enzymes. We further examined the roles of abnormal FAAH activity and AEA–CB1R signalling in the regulation of cocaine-associated memory formation and granule neuron dendritic structure alterations in the dDG through Western blotting, electron microscopy and immunofluorescence.

Results: In the present study, we found that cocaine induced a decrease in the level of FAAH in the dDG and increased the level of AEA. A high level of AEA activated cannabinoid type 1 receptors (CB1Rs) and further triggered CB1R signalling activation and granule neuron dendritic remodelling, and these effects were reversed by blockade of CB1Rs in the brain. Furthermore, inhibition of FAAH in the dDG markedly increased AEA levels and promoted cocaine-associated memory formation through CB1R signalling activation.

Conclusions: Together, our findings demonstrate that the lipase FAAH influences CB1R signalling activation and granule neuron dendritic structure alteration in the dDG by regulating AEA levels and that AEA and AEA metabolism play a key role in cocaine-associated memory formation. Manipulation of AEA production may serve as a potential therapeutic strategy for drug addiction and relapse prevention.

Keywords Cocaine-associated memory; Endocannabinoids; CB1R; Dorsal dentate gyrus; FAAH; AEA

1. INTRODUCTION

The risk of relapse is a major obstacle in treating the neuropsychiatric disease of drug addiction [1]. Exposure to drug-associated environmental stimuli triggers the retrieval of drug-associated memory, which can lead to drug craving and cause relapse [2]. Previous studies reported that targeted interference with cocaine-associated memory could suppress the propensity for drug relapse [3]. Thus, uncovering the underlying neurobiological mechanisms of drug-associated memory formation may reveal novel ways to improve drug addiction treatment and prevent relapse.

Brain endocannabinoids (eCBs) are primarily retrograde messengers that regulate synaptic plasticity [4] and memory formation through the stimulation of presynaptic cannabinoid type 1 receptors (CB1Rs) [5,6]. Some studies have reported that CB1R antagonist treatment during memory formation can disrupt heroin-, morphine-, methamphetamine- and nicotine-associated memory [7–10]. However, the precise mechanistic role of CB1Rs in drug-associated memory formation is not fully understood.

eCBs signalling in the brain relies primarily on metabotropic receptors, endogenous ligands, and enzymes that synthesize and degrade the ligands [11]. eCBs include anandamide (AEA) and 2-arachidonoyl

[1]National Chengdu Center for Safety Evaluation of Drugs, State Key Laboratory of Biotherapy/Collaborative Innovation Center for Biotherapy, West China Hospital, Sichuan University, Chengdu, China [2]Department of Pediatrics, Sichuan Academy of Medical Science & Sichuan Provincial People's Hospital, School of Medicine, University of Electronic Science and Technology of China, Chengdu, China [3]Acupuncture and Tuina School, Chengdu University of Traditional Chinese Medicine, Chengdu, Sichuan, China [4]Histology and Imaging Platform, Core Facilities of West China Hospital, Sichuan University, Chengdu 610041, China

[5] Hongchun Li and Rong Chen contributed equally to this work.

*Corresponding author. National Chengdu Center for Safety Evaluation of Drugs, State Key Laboratory of Biotherapy/Collaborative Innovation Center for Biotherapy, West China Hospital of Sichuan University, #1 Keyuan Road 4, Gaopeng Street, High-tech Development Zone, Chengdu 610041, China. E-mail: lihongchun0406@163.com (H. Li).

Received August 23, 2022 • Revision received September 6, 2022 • Accepted September 6, 2022 • Available online 9 September 2022

https://doi.org/10.1016/j.molmet.2022.101597

glycerol (2-AG), the most predominant ligand of CB1Rs. 2-AG is produced through the metabolism of 1,2-diacylglycerol by diacylglycerol lipase (DAGL) and is hydrolysed by monoacylglycerol lipase (MAGL). AEA, a primary brain endocannabinoid that directly binds to CB1Rs, is derived from the phospholipid precursor N-arachidonoyl-phosphatidylethanolamine (NAPE); the reaction is catalysed by a specific phospholipase D (NAPE-PLD). In addition, AEA is tightly regulated by the catabolic enzyme fatty acid amide hydrolase (FAAH), which plays an important role in regulating interstitial AEA levels in the synapse [12]. At present, eCBs are widely hypothesized to be involved in the brain pathways of reward behaviour, although this hypothesis is controversial [13]. For example, the CB1R antagonist AM251 inhibited the reinstatement of cocaine seeking [14], and the CB1R agonist WIN 55,212-2 also decreased cocaine self-administration [15]. Therefore, we need to further explore the role of brain eCBs in reward behaviour, especially their role in cocaine-associated memory formation.

It is well known that the hippocampus plays an important role in memory formation, and the dorsal dentate gyrus (dDG) is particularly involved in drug-associated memory formation [16,17]. Local inhibition of Fyn activity in the dDG prior to cocaine conditioned place preference (CPP) disrupted cocaine-associated memory formation, confirming that the dDG is an important region for cocaine-associated memory formation [17]. Hippocampal neuron synaptic plasticity is considered one of the primary mechanisms underlying learning and memory processes [18]. Several conceptualizations of addiction posit that the reinforcing and rewarding effects of drugs of abuse are caused by the "hijacking" of synaptic plasticity mechanisms, and abnormal synaptic plasticity mechanisms represent a powerful pathological form of learning and memory [4]. The eCBs system, one of the main endogenous systems controlling neuroplasticity within the hippocampus [19], can suppress neurotransmitter release at excitatory and inhibitory synapses. In addition, recent reports revealing that eCBs mediate retrograde synaptic signalling have unveiled a novel concept of how diffusible lipid ligands modify synaptic plasticity [20]. However, little is currently known about the mechanisms that regulate synaptic plasticity in the dDG through specific small neuromodulatory lipid ligand metabolism and further affect drug-associated memory formation.

In the present study, we reported that cocaine significantly activates CB1R signalling in the dDG of mice through high AEA production during cocaine-associated memory formation. Blocking the CB1R, the receptor to which AEA directly binds, could inhibit activation of the downstream CB1R signalling pathway and cocaine-induced granule neuron dendritic remodelling; these effects are necessary to disrupt cocaine-associated memory formation. Our findings shed light on the role of AEA in CB1R signalling activation and synaptic structure alteration during cocaine-associated memory formation; furthermore, our results show that eCBs may represent promising therapeutic targets for the treatment of cocaine addiction.

2. MATERIALS AND METHODS

2.1. Animals

Male C57BL/6 J mice (6−8 weeks old) were purchased from Vital River Laboratory Animal Technology Co., Ltd. (Beijing, China). All of the mice were housed in the animal facility under a standard 12-h light/12-h dark cycle at a constant room temperature. All experimental procedures and animal use protocols were in accordance with the guidelines established by the Association for Assessment and Accreditation of Laboratory Animal Care and the Institutional Animal Care and Use Committee of Sichuan University. All efforts were made to minimize the suffering of the mice.

2.2. Drugs

Cocaine was obtained from the National Institute for the Control of Pharmaceutical and Biological Products (Beijing, China) and dissolved in saline. Rimonabant (S3021, Selleck) was dissolved in saline containing 6% Tween 80; AM6545 (16,316, Cayman) was also dissolved in saline containing 6% Tween 80. AEA (90,050, Cayman) was dissolved in saline with 2% ethanol and 2% Tween 80. URB597 (S2631, Selleck) was dissolved in saline contain 0.1% DMSO.

2.3. Behavioural paradigm

Mice were acclimated to the laboratory environment for one week before experiments and habituated to handling for 2 d before each behavioural test. CPP was used to assess cocaine-associated memory formation. Food CPP and home-cage cocaine injection were employed as control behavioural tests. All behavioural experiments were performed in a double-blind manner.

2.3.1. CPP

The CPP test was conducted using a standard three-chambered apparatus equipped with two large conditioning compartments (black and white) that differed in their flooring (bar and grid) and a small middle chamber (grey, with a smooth PVC floor) that connected the two large compartments. Before each session, animals were habituated to the chambers for at least 10 min per day on 2 consecutive days.

2.3.2. Pre-test session

Baseline preference was assessed by placing the mice in the middle chamber and allowing them to explore all three chambers freely for 15 min, habituating to the apparatus as they did so. Baseline preference was calculated by subtracting the time spent in the black chamber from the time spent in the white chamber ($Time_{pre\text{-}test}$). Animals were excluded from the test if they showed a strong unconditioned preference for either side chamber (chamber bias $>$300 s or chamber bias $<-$300 s).

2.3.3. CPP training

Animals were randomly divided into two groups and trained for 6 d with alternating injections of cocaine (20 mg/kg or 2.5 mg/kg, i.p.) and saline. Cocaine-treated mice were immediately placed into the cocaine-paired chamber for 30 min after cocaine injection. On the following day, these mice received a saline injection and were immediately placed into the opposite chamber for 30 min. Saline-treated mice received an injection of saline and were placed into the vehicle-paired chamber for 30 min. On the following day, these mice received another saline injection and were placed in the opposite chamber for 30 min. The alternating sessions of conditioning were repeated until 3 cycles were complete (a total of 6 d). On the day of the test, the animals were placed in the middle compartment, and the time spent in the two compartments was recorded for 15 min. We defined the time spent in the black chamber minus the time spent in the white chamber as $Time_{test}$. The CPP score was calculated as the $Time_{test}$ test minus the $Time_{pre\text{-}test}$ (CPP score $= Time_{test} - Time_{pre\text{-}test}$). Generally, cocaine results in a positive CPP score and strongly reverses any preference to the contrary; the CPP score was defined as the extent of the shift in preference after cocaine injection.

2.3.4. Food CPP

The apparatus and methodology for the food CPP test were similar to those described above for cocaine CPP. Mice were food-restricted for one week before the test; their weight was maintained at 80% of their

original body weight. During the food conditioning sessions, the food conditioning group was transferred to the food-paired chamber (2–3 g of food was placed in the chamber) for 30 min. In the non-food conditioning sessions, mice were assigned to the non-food-paired chamber for 30 min. Outside of conditioning training, animals had access to food only once daily for 1 h, beginning 3 h after the training session ended. The alternating sessions of conditioning were repeated in 3 full cycles (a total of 6 d). On the day of the test, mice were placed in the central chamber and allowed to freely explore all three chambers for a total of 15 min; the time spent in each chamber was recorded to calculate the CPP score.

2.3.5. Home-cage cocaine injection

Mice were treated with cocaine as described in the procedure for cocaine CPP training, but they were not confined to the drug-paired chamber or the unpaired chamber after drug injection; instead, they were returned to their home cages without any exposure to the test apparatus. On the day of the test, mice were placed in the central chamber and allowed to freely explore all three chambers for a total of 15 min; the time spent in each chamber was recorded to evaluate the CPP score.

2.4. Tissue isolation

Mice were killed by rapid decapitation immediately following the cocaine CPP testing. The dDG was removed from the brain, snap-frozen in liquid nitrogen, and stored at −80 °C until the assay.

2.5. UPLC/Q-TOF MS/MS for AEA and 2-AG detection

Brain tissue was collected immediately following cocaine preference testing and was prepared by using an ethyl acetate/hexane (9:1, v/v) extraction method adapted from a previously published study [21]. Tissues were spiked with ethyl acetate/hexane and internal standards (d4-AEA (10011178, Cayman) at 10 μg/mL; d5-2-AG (362,162, Cayman) at 100 μg/mL; 2 μL of mixed internal standards for each sample) and ultrasonicated in an ice-cold water bath. Then, the mixture was diluted with ∼10% of its volume of water and transferred to a centrifugation tube. Samples were centrifuged at 7000×*g* at 4 °C for 15 min, and the supernatants were transferred to clean tubes. The homogenization and centrifugation steps were repeated three times, with the supernatants pooled to optimize AEA and 2-AG recovery. Then, the pooled supernatants were evaporated to dryness under a gentle stream of nitrogen.

The dry residue was dissolved in 50 μL acetonitrile, and 5 μL reconstituted extract was injected into the LC/MS–MS system for analysis. Chromatographic separation was performed using a Waters ACQUITY UPLC system (Waters Corp., Milford, USA) with a reversed-phase ACQUITY UPLC HSS T3 column (2.1 mm × 100 mm × 1.8 μm) maintained at 40 °C by gradient elution with a mobile phase flow rate of 0.3 mL/min. The gradient elution mobile phases consisted of A (acetonitrile with 0.1% formic acid) and B (water with 0.1% formic acid).

MS/MS analyses were accomplished in positive ion mode with electrospray ionization (ESI) using Xevo G2-S Q-TOF (Waters Corp., Milford, USA). For targeted MS/MS scans, the cone voltage was set to 30 V for AEA and d4-AEA; a voltage of 10 V was used for 2-AG and d5-2-AG. LE was applied to ensure the *m/z* accuracy of the mass spectrometer, and sodium formate solution was used to calibrate the TOF function of the mass spectrometer. A comparison of the paired ion (precursor and product ion *m/z* values) and LC retention times with standards served to confirm the identification of the two lipids. The ion pairs were 348.2903/131.0946 for AEA, 379.2848/361.2748 for 2-AG, 352.3154/135.1197 for d4-AEA, and 384.3162/366.3057 for d5-2-AG. 2-AG is chemically unstable in aqueous solutions and is likely to form 1-AG by molecular rearrangement. We thus calculated the amount of 2-AG by summing the measured quantities of 2-AG and 1-AG. Data acquisition and processing were accomplished using MassLynx (Waters Corp).

2.6. Western blotting

After cocaine CPP testing, the brain tissue was harvested immediately and was lysed and proteins extracted using a mammalian cell and tissue extraction kit (K269-500, Biovision) containing phosphatase inhibitors (4906845001, Roche) according to the manufacturer's protocols. The total protein concentration was analysed with a Bradford assay kit (P0006, Beyotime). Twenty micrograms of protein was loaded and separated on 10% or 12.5% sodium dodecyl sulfate-polyacrylamide gels. After the proteins were separated, they were transferred from the gels to polyvinylidene difluoride membranes (IPVH00010, Millipore) in a mixed solution of Tris-glycine buffer and 20% (v/v) methanol. The membrane was blocked in TBST buffer containing 5% non-fat dry milk (9999, Cell Signaling Technology) for 1 h at room temperature, then incubated and gently shaken overnight with the primary antibody at 4 °C. On the next day, after three washes with TBST for 15 min, the blots were incubated with the secondary antibody at room temperature for 2 h. Immunoreactivity was visualized using a chemiluminescence substrate (WBKLS0500, Millipore) and a chemiluminescence imaging system (CLINX). The optical density of each band was quantified using Chemi Analysis software (CLINX). The following antibodies were used for Western blotting: rabbit anti-FAAH (1:1000, Abcam), rabbit anti-NAPE-PLD (1:1000, Abcam), mouse anti-CB1R (1:1000, Abcam), rabbit anti-DAGL-α (1:1000, Abcam), rabbit anti-DAGL-β (1:1000, Abcam), goat anti-MAGL (1:1000, Abcam), rabbit anti-Synaptophysin (1:1000, Abcam), mouse anti-PSD95 (1:1000, Abcam), rabbit anti-Cofilin (1:1000, Abcam), rabbit anti-Drebrin (1:1000, Proteintech), rabbit anti-extracellular signal regulated kinase (ERK) 1/2 (1:1000, Cell Signaling Technology), rabbit anti-p-ERK1/2 (T 202/T 204; 1:1000, Cell Signaling Technology), rabbit anti-mTOR (1:1000, Cell Signaling Technology), rabbit anti-p-mTOR (1:1000, Cell Signaling Technology), mouse anti-GAPDH (1:2000, ZSGBBIO), goat anti-mouse (HRP; Invitrogen), and goat anti-rabbit (HRP; Invitrogen).

2.7. Stereotactic surgery and inhibitor administration

Animals were anaesthetized with sodium pentobarbital (60 mg/kg) and mounted in a standard stereotaxic instrument (RWD Life Science). The hair was shaved from the planned incision site on the scalp, and the site was cleaned with medical-grade alcohol. The scalp was incised to expose the skull, and permanent bilateral guide cannulas (RWD Life Science) were implanted into the dDG (AP, −2.0 mm; ML, ±1.4 mm; DV, −2.2 mm) with stereotaxic instruments. Dental cement was used to anchor the guide cannula, and a stainless-steel stylet was left in each cannula to prevent blockage and infection. All mice began training after one week of recovery from surgery.

Beginning 30 min before cocaine or saline administration, rimonabant and AM6545 (0.6 μg/μL, 1 μL/side, 0.5 μL/min) [21] as well as URB597 (10 ng/μL, 1 μL/side, 0.5 μL/min) [22] were administered bilaterally with a micro-injector. Beginning 15 min before cocaine or saline treatment, AEA (10 μM/side, 0.5 μL/min) was injected.

2.8. Measurement of FAAH activity

After the cocaine CPP testing, we collected the brain tissue immediately. According to the manufacturer's instructions, FAAH activity in the

dDG was measured with an FAAH inhibitor screening assay kit (10005196, Cayman).

2.9. In vivo cellular fluorescent labelling

Single-cell fluorescent labelling was performed as previously described with slight modifications [23]. Briefly, mice (8−12 weeks old) were anaesthetized with sodium pentobarbital (60 mg/kg) and placed on a stereotaxic apparatus (RWD Life Science), and the dDG (AP, −2.0 mm; ML, ±1.4 mm; DV, −2.2 mm) was injected with the appropriate viral vectors. Specifically, microsyringes were used to bilaterally infuse a mixture of adeno-associated viruses (AAVs) pAAV-Syn-DIO-(tTA-P2A-mNeonGreen)-WPRE (Obio Technology Co., Ltd., Shanghai, China) and pAAVPTRE-tight-NLS-Cre (Obio Technology Co., Ltd., Shanghai, China) into the brain at a rate of 0.05 μL/min for 10 min (0.5 μL per side). After each injection, the syringe was left in place for an additional 5 min and then slowly withdrawn to allow diffusion of the viruses. The mice were allowed to recover for at least 3 weeks before cocaine CPP training.

After cocaine CPP training, the animals were deeply anaesthetized with sodium pentobarbital (60 mg/kg) and perfused transcardially with phosphate-buffered saline (PBS) followed by ice-cold 4% paraformaldehyde in 0.1 M PBS (pH 7.4). We carefully extracted the brains from the skulls, postfixed them with 4% PFA overnight, and then dehydrated them in 30% sucrose at 4 °C. We sectioned the brains into 50-μm-thick coronal slices using a freezing microtome (Leica, Germany), mounted them on slides, dried them and stored them at −80 °C until we processed them for immunohistochemistry.

Sections were washed with PBS 3 times for 10 min each and covered with anti-fade mounting medium with DAPI (H-1200, Vector). A laser confocal microscope (Nikon, Japan) was used to acquire brain images. Each neuron was scanned at high magnification (100×, oil immersion lens) to ensure that all parts of the dendrites were intact. A minimum of 3 neurons per slice from each group were examined, and at least 40 neurons were selected from each group. Confocal microscopy was performed for the 3D reconstruction of neurons. The total dendritic length and dendritic spine density were measured using ImageJ software (US National Institutes of Health, Bethesda, MD, United States).

2.10. Transmission electron microscopy

When mice finished the cocaine CPP testing, they were deeply anaesthetized with sodium pentobarbital injection (60 mg/kg) and intracardially perfused with 50 mL of freshly prepared fixative containing 2.5% glutaraldehyde and 2% paraformaldehyde in 0.1 M PBS (pH 7.4). Whole brains were removed, postfixed with 2.5% glutaraldehyde overnight at 4 °C, impregnated with 1% osmium tetroxide for 1 h, dehydrated in graded alcohol solutions, flat embedded in Durcupan ACM (Fluka) and cured for 48 h at 60 °C. Small pieces containing the hippocampal dDG were removed from the specimens and glued onto a plastic block with cyanoacrylate. Ultrathin sections were cut and mounted on Formvar-coated single-slot grids. A transmission electron microscope (JEOL, Japan) was used to observe the synaptic structure. We obtained 5 images of each section, yielding at least 50−70 synapses from each mouse. Image-Pro Plus 6.0 software (US National Institutes of Health, Bethesda, MD, United States) was used for the morphometric analysis.

2.11. Statistical analysis

All data were analysed with GraphPad Prism 7 software and are presented as the means ± SEMs. The distribution of the data was tested for normality using the Kolmogorov−Smirnov test. An unpaired two-tailed Student's t test was used for simple pairwise comparisons. One-way or two-way ANOVA followed by the Bonferroni post hoc test was utilized for multiple comparisons. In all results, n refers to the number of animals. For all results, statistical significance was defined by $p < 0.05$.

3. RESULTS

3.1. Disordered AEA metabolism in the dDG after cocaine CPP training

The CPP test, an associative memory model linking a drug reward with environmental cues, is widely used to assess the formation of drug-associated memory [24,25]. In the present study, we first explored the effect of cocaine on the level of eCBs in the dDG during cocaine-associated memory formation. The timeline of the cocaine CPP training procedure is shown in Figure 1A. During habituation to the CPP apparatus, neither group showed a side preference. In the training phase, cocaine induced a significant increase in the CPP score (Figure 1B; $t_{(22)} = 4.757$, $p < 0.0001$). Next, we measured the AEA-metabolizing enzymes NAPE-PLD and FAAH by immunoblotting. Notably, the level of the AEA catabolic enzyme FAAH was significantly decreased by cocaine in the dDG, but the same was not true of NAPE-PLD (Figure 1C; FAAH: $t_{(10)} = 2.857$, $p < 0.05$). However, the levels of CB1R, 2-AG synthetase (DAGLα and DAGLβ) and catabolic enzymes (MAGL) were also not changed by cocaine (Figure 1C).

We continued to employ targeted ultra-high-performance liquid chromatography tandem mass spectrometry (UPLC/MS/MS) to quantitatively validate the changes in eCB lipid molecules (AEA and 2AG) in the dDG after cocaine CPP training. Deuterated AEA (d4-AEA) and deuterated 2-AG (d5-2-AG) were used as internal standards for comparison and confirmed that the alterations in 2-AG and AEA were specific. Compared with the saline group, the level of AEA was significantly increased in the cocaine group, but the same was not true of 2-AG (Figure 1D; AEA: $t_{(10)} = 2.648$, $p < 0.05$). We further assayed the direct effect of cocaine on FAAH activity using an ELISA, and the results demonstrated that FAAH activity was decreased after cocaine CPP training (Figure 1E; $t_{(7)} = 2.471$, $p < 0.05$). Thus, these results show that AEA is the predominant lipid molecule regulated by cocaine, and the increase in AEA may be mainly attributable to the decreased level and activity of FAAH, the key enzyme that hydrolyses AEA.

Previous studies have shown that eCBs contribute to ketamine-mediated dendritic remodelling in the neurons [21], and changes in dDG granule neuron structure play a critical role in regulating cocaine-associated memory formation [16]. We thus explored whether the dendritic structures of granule neurons were altered after cocaine CPP training. We performed immunoblotting to analyse the expression of proteins related to synaptic structure. The levels of Synaptophysin, PSD95 and Cofilin were markedly upregulated after cocaine CPP training (Figure 1F; Synaptophysin: $t_{(10)} = 2.895$, $p < 0.05$; PSD95: $t_{(10)} = 3.85$, $p < 0.01$; Cofilin: $t_{(10)} = 2.25$, $p < 0.05$). We next analysed the dendritic complexity of granule neurons using ImageJ and the Sholl analysis plugin, as described previously [21]. Our results showed that cocaine significantly enhanced the dendritic complexity of hippocampal granule neurons, increasing spine density, dendritic length and dendritic arborization (Figure 1G−J; spine density: $t_{(4)} = 3.113$, $p < 0.05$; dendritic length: $t_{(4)} = 3.186$, $p < 0.05$; intersection number: treatment $F_{(3.058,\ 12.23)} = 509.6$, $p < 0.0001$; distance from soma $F_{(1,\ 4)} = 204.1$, $p < 0.001$; interaction $F_{(25,\ 100)} = 6.031$, $p < 0.0001$). Collectively, our results indicated that cocaine-associated memory formation may contribute to remodelling the dendritic structure of the granule neurons in the dDG.

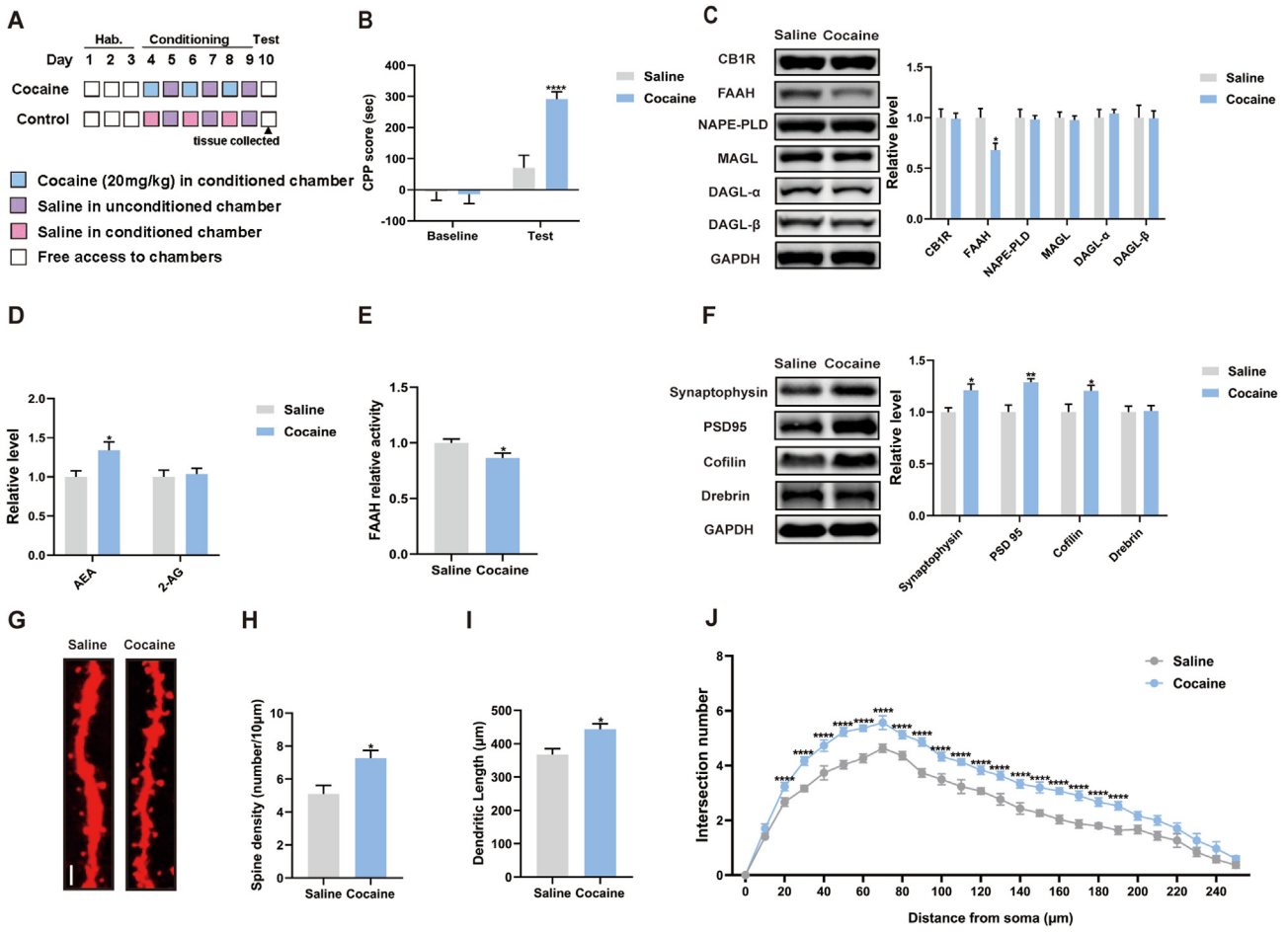

Figure 1: AEA level and dendrite structure remodeling in dDG are significantly increased during cocaine-associated memory formation. (A) Experimental timeline for cocaine CPP test. (B) CPP score was increased after cocaine CPP training (n = 12 per group). (C) Immunoblotting was analyzed expression of CB1R, FAAH, NAPE-PLD, MAGL, DAG-α and DAG-β in the dDG of mice (n = 6 per group). (D) The level of AEA and 2-AG in the dDG were detected after cocaine CPP training (n = 6 per group). (E) Cocaine significantly lower FAAH activity in the dDG of mice (n = 5 for saline group; n = 4 for cocaine group). (F) The level of Synaptophysin, PSD95, Cofilin and Drebrin were detected by western blot (n = 6 per group). (G) Representative images of dendritic spines in hippocampal neurons (100 × oil lens), Scale bars: 10 μm. (H) The spine density was elevated by cocaine (n = 3 per group). (I) The dendritic length was promoted by cocaine (n = 3 per group). (J) Cocaine induced dendritic arborization upregulation (n = 3 per group). Data are mean ± SEM, unpaired t test or two-way ANOVA, $*p < 0.05$, $**p < 0.01$ and $****p < 0.0001$. Hab, Habituation.

To further determine whether the changes in eCBs were specific to cocaine CPP memory formation, we performed two other reward tests, the food CPP test and the home-cage cocaine injection test (Supplementary Figs. 1A and 2A). In the former test, mice were exposed to a palatable food reward to train the food-associated cue memory but were not administered cocaine. In the latter test, mice were injected with cocaine but did not receive cocaine-associated cue training. Surprisingly, although food induced a significant increase in the CPP scores of the food-restricted mice (Supplementary Fig. 1B; $t_{(16)} = 2.554$, $p < 0.05$), changes in the levels of eCB-metabolizing enzymes and eCB lipid molecules were not observed in the dDG of the mice subjected to food CPP training (Supplementary Figs. 1C–D). In addition, the spine density and dendritic length of granule neurons were not altered after food CPP training (Supplementary Figs. 1E–G). In the home-cage cocaine injection test, cocaine failed to induce a significant increase in the CPP score (Supplementary Fig. 2B). The levels of eCB-metabolizing enzymes and FAAH activity in the dDG were not changed after home-cage cocaine injection (Supplementary Figs. 2C–D). Similarly, the levels of proteins related to synaptic structure, the density of dendritic spines, and the dendritic length of granule neurons were also not changed in the dDG of the mice subjected to home-cage cocaine injection (Supplementary Figs. 2E–H). These results suggested that the role of eCBs in the dDG may be specific to cocaine-associated memory formation.

3.2. CB1R blockade disrupts cocaine-associated memory formation

CB1Rs are highly expressed in presynaptic terminals in the hippocampus [19], and AEA and 2-AG primarily regulate synaptic transmission and plasticity via retrograde signalling to presynaptic CB1Rs [26]. Regarding the high level of AEA in the dDG after cocaine CPP training, we speculated that AEA–CB1R signalling may mediate cocaine-associated memory formation. To test this conjecture, we used rimonabant, an inverse agonist, to explore the role of CB1Rs in regulating cocaine-associated memory formation.

By administering rimonabant directly into the dDG, we tested the effect of CB1R blockade on cocaine-associated memory formation. After a week of recovery from cannulation surgery, mice underwent cocaine CPP training (Figure 2A), and rimonabant was delivered into the dDG half an hour before each training session. The results of behavioural

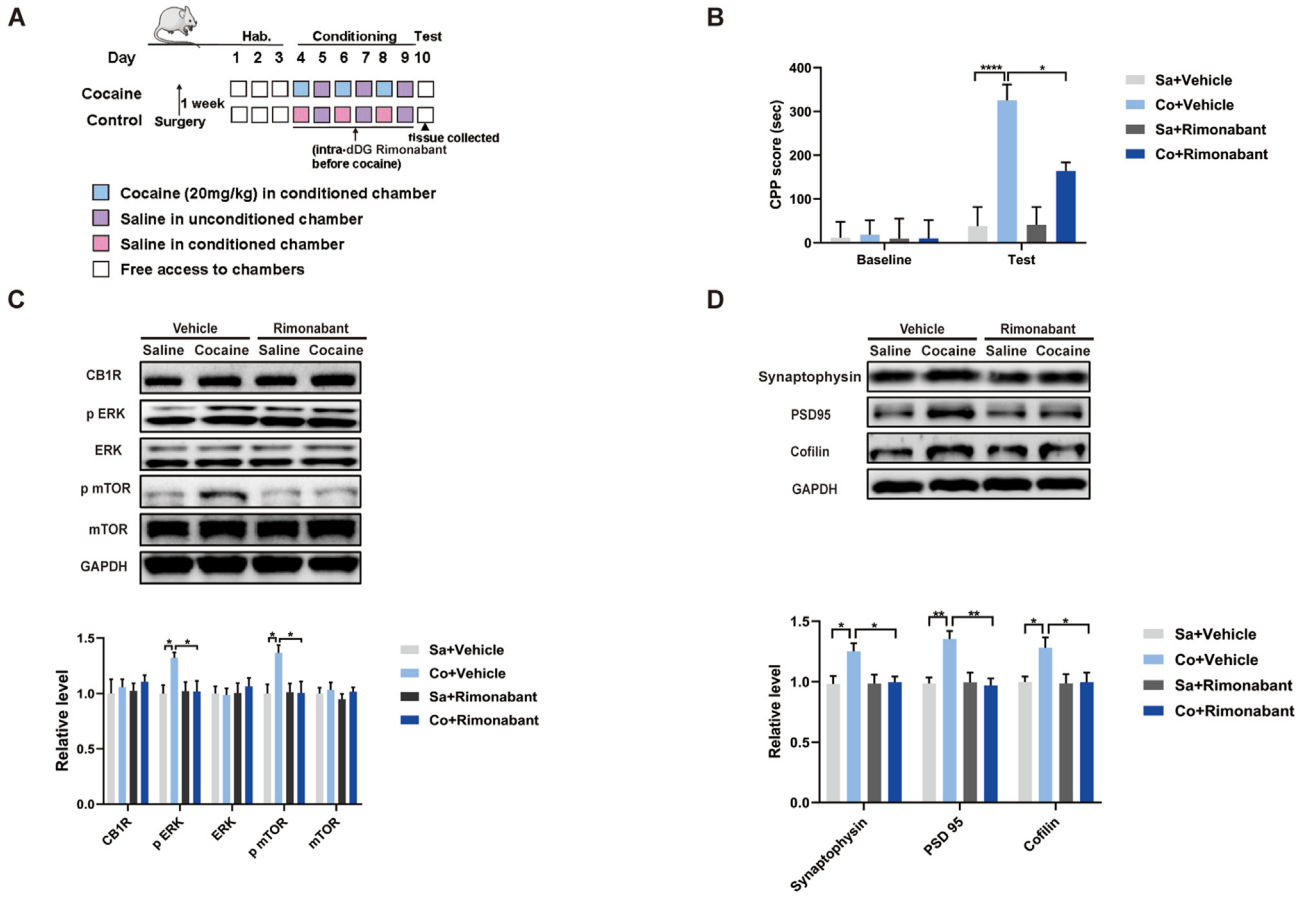

Figure 2: CB1Rs blockage suppresses the cocaine-associated memory formation and downstream signaling molecular activation. (A) Experimental time course for cocaine-associated memory formation in the mice receiving intra-dDG infusion of rimonabant. (B) Bilateral intra-dDG infusion of rimonabant attenuated cocaine CPP score (n = 8 for Sa + Vehicle group; n = 8 for Co + Vehicle group; n = 9 for Sa + Rimonabant group; n = 8 for Co + Rimonabant group). (C) Immunoblotting was detected the downstream signaling molecules after CB1Rs blockage (n = 6 per group). (D) The level of Synaptophysin, PSD95 and Cofilin were detected by western blot (n = 6 per group). Data are mean ± SEM, one-way ANOVA, $*p < 0.05$, $**p < 0.01$ and $****p < 0.0001$. dDG, dorsal dentate gyrus; Sa, Saline; Co, Cocaine.

tests showed that intra-dDG infusion of rimonabant clearly reduced CPP scores (Figure 2B; $F_{(3, 28)} = 13.85$, $p < 0.0001$), suggesting that CB1R activation plays an important role in cocaine-associated memory formation.

To further elucidate the downstream intracellular pathways involved in the effects of CB1R blockade, we used immunoblotting to study the expression of ERK and phosphorylated ERK (p-ERK), key regulators of synaptic plasticity [27]. In addition, activation of CB1R triggers mammalian target of rapamycin (mTOR) signalling in the hippocampus [28]; we quantified phosphorylated (active) mTOR in both saline- and cocaine-treated mice. Notably, cocaine increased the levels of both p ERK and p mTOR, and these effects were reversed by rimonabant, while the expression levels of CB1R, ERK and mTOR were not altered by either cocaine or rimonabant administration (Figure 2C; p ERK: $F_{(3, 20)} = 3.978$, $p < 0.05$; p mTOR: $F_{(3, 20)} = 4.45$, $p < 0.05$), indicating that high AEA content in the dDG of cocaine mice may activate intracellular pathways downstream of the CB1R.

3.3. Granule neuron dendrite structure is altered via CB1Rs in the dDG during cocaine-associated memory formation

We next performed immunoblotting to analyse the expression of synaptic proteins in the dDG of the mice subjected to intra-dDG infusion of rimonabant during cocaine CPP training; we found that cocaine enhanced the expression of Synaptophysin, PSD95, and Cofilin, and these effects were clearly attenuated by intra-dDG infusion of rimonabant (Figure 2D; Synaptophysin: $F_{(3, 20)} = 4.362$, $p < 0.05$; PSD95: $F_{(3, 20)} = 8.369$, $p < 0.001$; Cofilin: $F_{(3, 20)} = 4.048$, $p < 0.05$). We continued to observe the dendritic complexity of granule neurons in the dDG using ImageJ software and the Sholl analysis plugin. The morphology results showed that rimonabant reversed the cocaine-induced increases in dendritic length, spine density and dendritic complexity (Figure 3A–D; spine density: $F_{(3, 8)} = 11.29$, $p < 0.01$; dendritic length: $F_{(3, 8)} = 14.84$, $p < 0.01$; intersection number: treatment $F_{(25, 208)} = 804.4$, $p < 0.0001$; distance from soma $F_{(3, 208)} = 184.9$, $p < 0.0001$; interaction $F_{(75, 208)} = 2.807$, $p < 0.0001$). We also performed electron microscopy to observe synaptic alterations during cocaine-associated memory formation. An analysis of dDG synapses in cocaine-treated mice revealed significant increases in the density and length of the postsynaptic density (PSD) (Figure 3E–G), whereas no alteration in the thickness (a measure of maturation) of the PSD was observed between the cocaine-treated group and the control group (Figure 3H). However, this increase was considerably attenuated by intra-dDG rimonabant injection (Figure 3E–G; PSD density: $F_{(3, 8)} = 9.843$, $p < 0.01$; PSD length: $F_{(3, 8)} = 14.35$, $p < 0.01$). Collectively, our results indicated that CB1R activation may contribute to cocaine-induced granule neuron dendritic remodelling in the dDG.

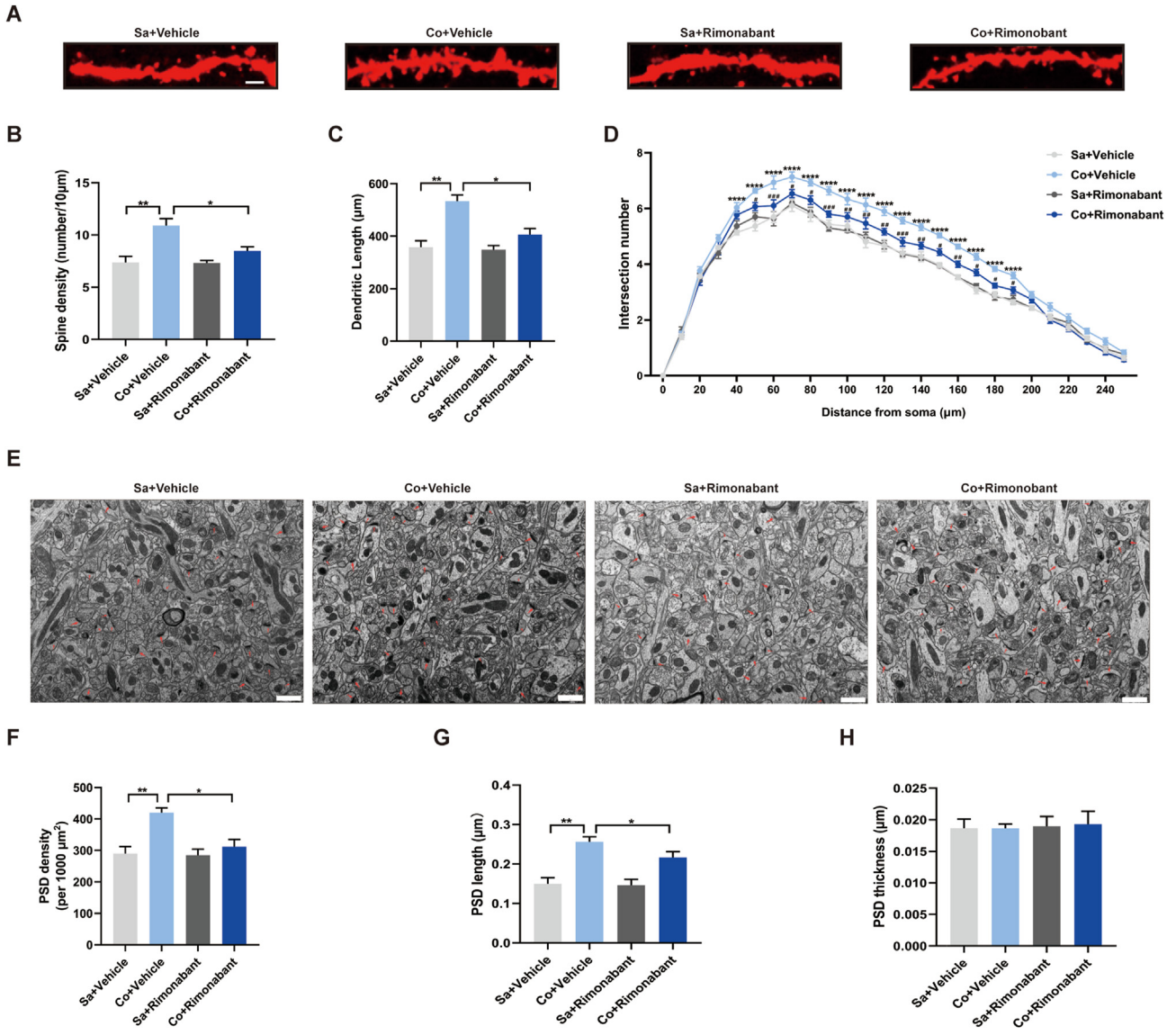

Figure 3: Cocaine-induced dendrite structure in dDG in cocaine CPP model by a CB1R-dependent manner. (A) Representative images of dendritic spines in hippocampal neurons (100 × oil lens), the scale bar is 10 μm. (B–D) CB1R blockage attenuated spine density, dendritic length and dendritic arborization increased by cocaine (n = 3 per group). (E) Representative TEM images of dDG synapses, red arrows refer to synapses, the scale bar is 1 μm. (F–H) PSD density and length, but not thickness, were decreased in the hippocampal dDG after rimonabant pretreatment, as determined by electron microscopy analysis (n = 3 per group). Data are mean ± SEM, one-way or two-way ANOVA, compared to Sa + Vehicle group $^{*}p < 0.05$, $^{**}p < 0.01$ and $^{****}p < 0.0001$; compared to co + Vehicle group $^{\#}p < 0.05$, $^{\#\#}p < 0.01$ and $^{\#\#\#}p < 0.001$. TEM, Transmission electron microscopy.

3.4. Central AEA–CB1R signalling is necessary for cocaine-induced granule neuron dendritic remodelling in the dDG during cocaine-associated memory formation

To explore whether brain AEA–CB1R signalling regulates the sensitivity of cocaine-associated memory formation, we subjected all mice to low-dose (2.5 mg/kg) cocaine CPP training. After a week of recovery from cannulation surgery, mice were trained to develop cocaine CPP; rimonabant or AM6545 was delivered into the dDG half an hour before each training session, and AEA was delivered into the dDG 15 min before training (Figure 4A). Interestingly, mice injected with AEA in the dDG showed increased CPP scores, while pretreatment with rimonabant clearly attenuated these effects regardless of whether AEA was infused (Figure 4B). To further assess the relative contributions of central and peripheral AEA–CB1R signalling to cocaine-associated memory formation, we compared the effects of rimonabant to the effects of AM6545, a CB1R antagonist with a limited ability to cross the blood–brain barrier. In contrast to rimonabant, AM6545 did not reverse the AEA-induced increase in sensitivity to cocaine-associated memory formation (Figure 4B; $F_{(5, 48)} = 13.27$, $p < 0.0001$), indicating that central AEA–CB1R signalling is necessary to promote cocaine-associated memory formation, at least under the conditions of our study. In addition, we confirmed that mice pre-treated with AEA showed a significant increase in the dDG levels of p ERK and p mTOR compared with control mice, and this effect of AEA was strictly dependent on CB1R activation, as it was reversed by rimonabant. However, AM6545

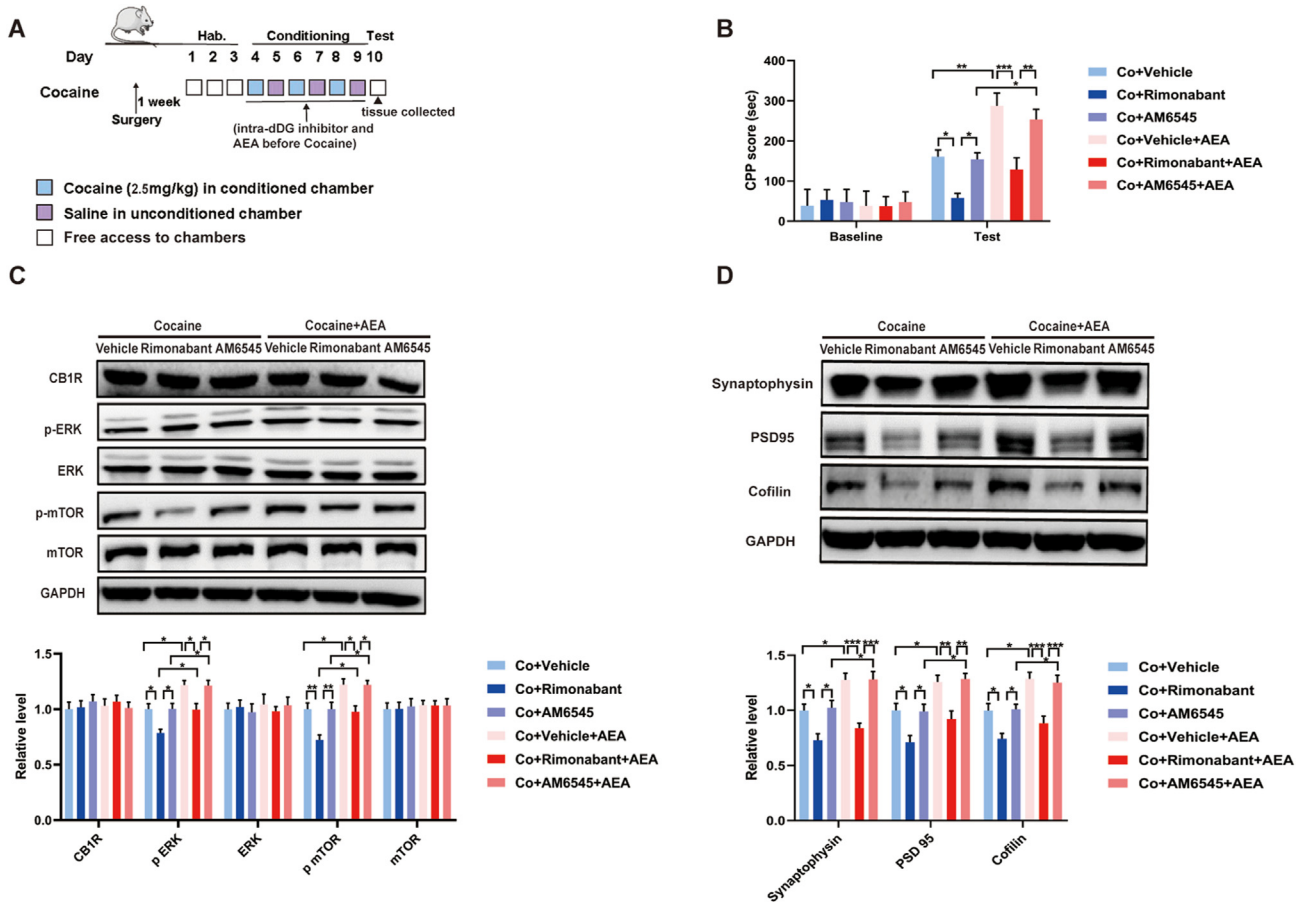

Figure 4: AEA is necessary for cocaine-associated memory formation by activation central CB1Rs. (A) Experimental time course for cocaine CPP training and after intra-dDG infusion of CB1R inhibitors and AEA. (B) Intra-dDG infusion of AEA obviously promoted the cocaine-associated memory formation and such effects were attenuated by CB1R central inhibitor (n = 9 per group). (C) Immunoblotting was detected the downstream signaling molecules after cocaine CPP training (n = 6 per group). (D) The level of Synaptophysin, PSD95 and Cofilin were detected by western blot (n = 6 per group). Data are mean ± SEM, one-way ANOVA, $*p < 0.05$, $**p < 0.01$ and $***p < 0.001$.

administration failed to reverse these effects of AEA (Figure 4C). Similarly, the expression levels of CB1R, ERK and mTOR were significantly altered by the administration of either an AEA or a CB1R inhibitor (Figure 4C; p ERK: $F_{(5,\ 30)} = 12.04$, $p < 0.0001$; p mTOR: $F_{(5,\ 30)} = 12.56$, $p < 0.0001$).

Regarding the expression of synaptic proteins, immunoblot results showed that AEA induced a significant upregulation of Synaptophysin, PSD95, and Cofilin, and such effects were also markedly reversed by rimonabant but not by AM6545 (Figure 4D; Synaptophysin: $F_{(5,\ 30)} = 13.74$, $p < 0.0001$; PSD95: $F_{(5,\ 30)} = 11.74$, $p < 0.0001$; Cofilin: $F_{(5,\ 30)} = 12.99$, $p < 0.0001$). Furthermore, when we observed the dendritic complexity of granule neurons in the dDG, we found that rimonabant reversed the AEA-induced increase in dendritic length and spine density and that AM6545 was unable to reverse these effects (Figure 5A–C; spine density: $F_{(5,\ 12)} = 137.8$, $p < 0.0001$; dendritic length: $F_{(5,\ 12)} = 31.26$, $p < 0.0001$). We continued to observe synaptic alterations in the dDG after pre-treatment with AEA. We found that AEA increased the density and length of the PSD after low-dose cocaine CPP training, and these effects were blocked by rimonabant but not AM6545, whereas no alteration in the thickness of the PSD was observed (Figure 5D–G; PSD density: $F_{(5,\ 12)} = 81.31$, $p < 0.0001$; PSD length: $F_{(5,\ 12)} = 38.25$, $p < 0.0001$). Remarkably, our data strongly demonstrate that brain AEA–CB1R signalling is necessary for cocaine-induced dendritic remodelling in granule neurons during cocaine-associated memory formation.

3.5. FAAH is essential for cocaine-associated memory formation

The level of AEA is tightly regulated by the catabolic enzyme FAAH [29]. FAAH is highly expressed in the brain regions implicated in reward and addiction [12]. To explore how FAAH affects cocaine-associated memory formation, we injected the FAAH inhibitor URB597 into the bilateral dDG of mice during low-dose cocaine CPP training (Figure 6A). Compared with the vehicle control, URB597 significantly increased the CPP scores of treated mice (Figure 6B; $F_{(3,\ 32)} = 7.842$, $p < 0.001$), indicating that inhibition of FAAH could promote cocaine-associated memory formation. In addition, FAAH activity was significantly decreased after URB597 treatment (Figure 6C; $F_{(3,\ 12)} = 8.856$, $p < 0.01$). We observed the downstream intracellular pathways involved in the effects of CB1R activation after FAAH inhibition. Immunoblot results demonstrated that the levels of p ERK and p mTOR were significantly increased after URB597 administration during low-dose cocaine CPP training (Figure 6D; p ERK: $F_{(3,\ 20)} = 4.552$, $p < 0.05$; p mTOR: $F_{(3,\ 20)} = 8.840$, $p < 0.001$), indicating that FAAH may mediate CB1R activation.

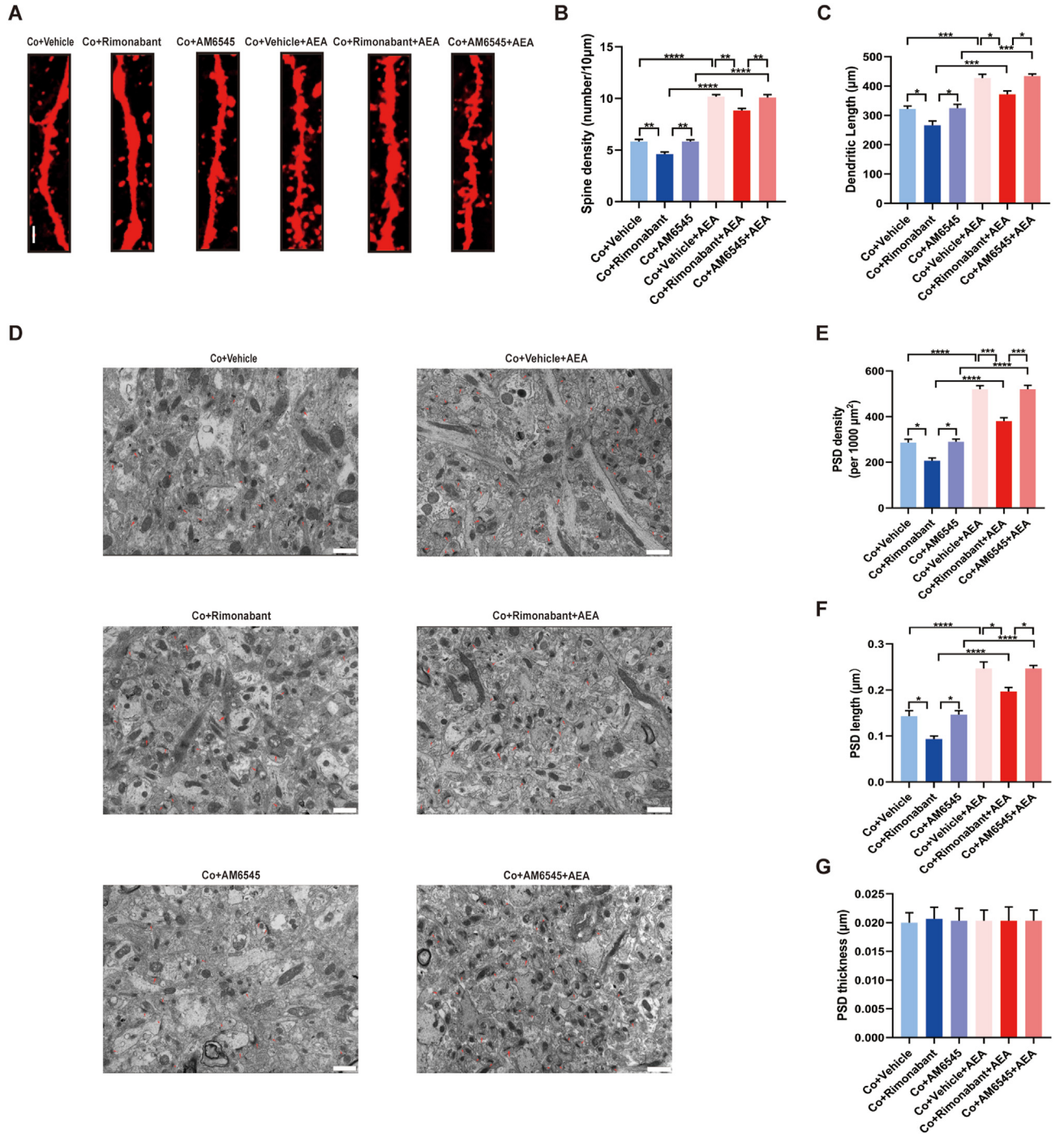

Figure 5: AEA is necessary for cocaine-associated memory formation by alteration dendrite structure. (A) Representative images of dendritic spines in hippocampal neurons (100 × oil lens), the scale bar is 10 μm. (B–C) Intra-dDG infusion of AEA obviously promoted the cocaine-induced spine density and dendritic length, and such effects were attenuated by CB1R central inhibitor (n = 3 per group). (D) Representative TEM images of dDG synapses, red arrows refer to synapses, the scale bar is 1 μm. (E–G) Intra-dDG infusion of AEA increased the PSD density and length, and such effects were decreased by CB1R central inhibitor (n = 3 per group). Data are mean ± SEM, one-way ANOVA, $*p < 0.05$, $**p < 0.01$, $***p < 0.001$ and $****p < 0.0001$.

Finally, we investigated whether FAAH inhibition promoted granule neuron dendritic complexity in the dDG. Western blot results showed that the levels of the synaptic proteins Synaptophysin, PSD95, and Cofilin level were markedly increased after FAAH inhibition (Figure 6E; Synaptophysin: $F_{(3,\ 20)} = 5.528$, $p < 0.01$; PSD95: $F_{(3,\ 20)} = 4.804$, $p < 0.05$; cofilin: $F_{(3,\ 20)} = 6.027$, $p < 0.01$). Furthermore, URB597 significantly enhanced granule neuron dendritic complexity, promoting dendritic length and spine density (Figure 6F–H; spine density: $F_{(3,\ 8)} = 6.524$, $p < 0.05$; dendritic length: $F_{(3,\ 8)} = 7.996$, $p < 0.01$), suggesting that FAAH reinforced CB1R activation-induced dendritic

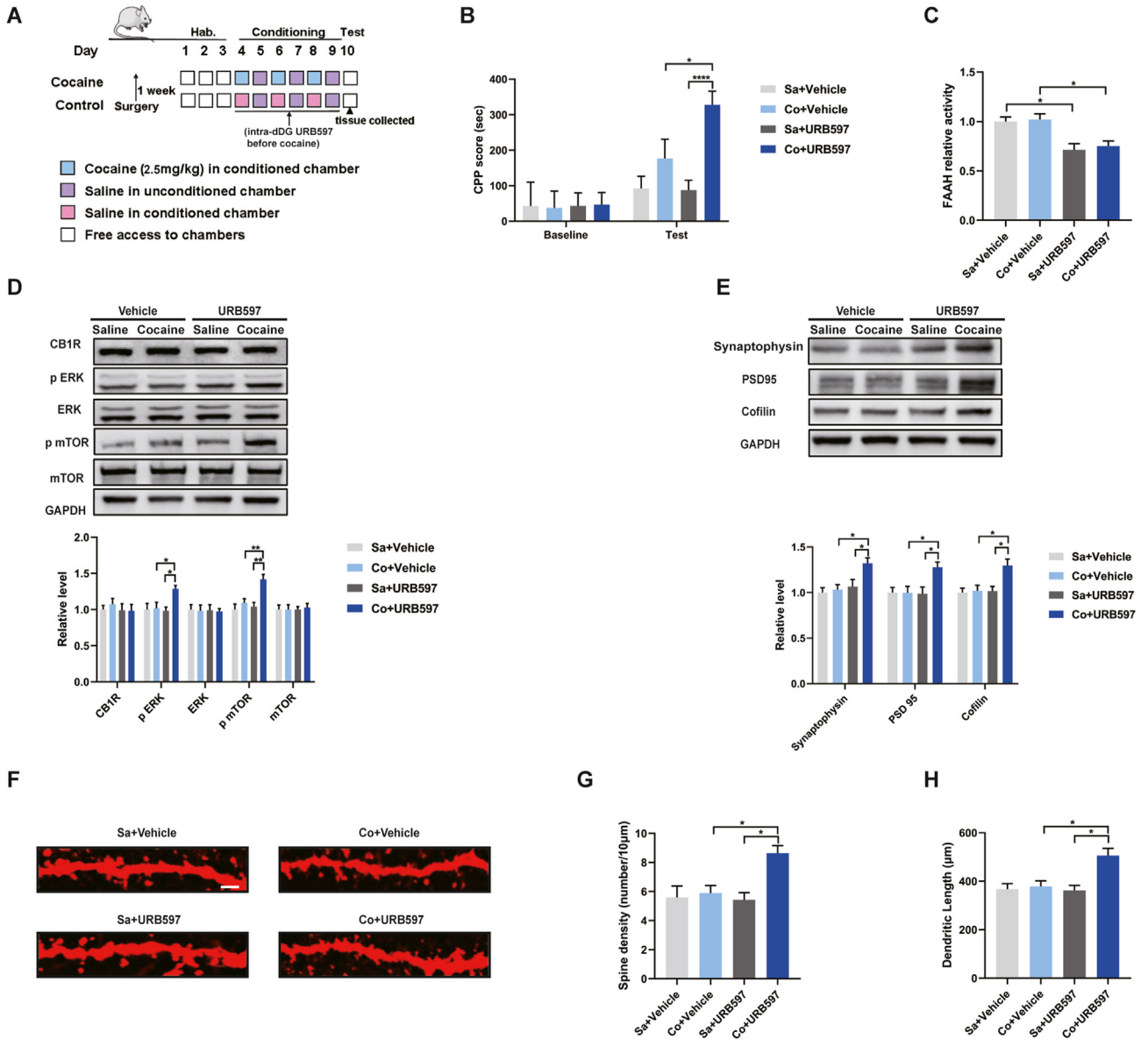

Figure 6: Inhibition of FAAH in the dDG promote cocaine-associated memory formation. (A) Experimental time course for intra-dDG injection of URB597 before cocaine CPP training. (B) Inhibition of FAAH obviously promoted the cocaine-associated memory formation (n = 9 per group). (C) FAAH activity was decreased after URB597 treatment (n = 4 per group). (D) Immunoblotting was detected the CB1R downstream signaling molecules during the cocaine CPP training (n = 6 per group). (E) The level of Synaptophysin, PSD95 and Cofilin were detected by western blot (n = 6 per group). (F) Representative images of dendritic spines in hippocampal neurons (100 × oil lens), the scale bar is 10 μm. (G–H) Inhibition of FAAH increased the spine density and length of granule neurons in dDG during the cocaine-associated memory formation (n = 3 per group). Data are mean ± SEM, one-way ANOVA, $*p < 0.05$, $**p < 0.01$ and $****p < 0.0001$.

remodelling in the dDG, which contributed to cocaine-associated memory formation.

4. DISCUSSION

Regarding eCBs signalling in the dDG of cocaine mice, AEA, but not 2-AG, plays an important role in cocaine-associated memory formation by triggering CB1Rs. In addition, cocaine decreases FAAH levels and leads to an increased level of AEA, further activating CB1R signalling and remodelling the dendritic spine structure of granule neurons, which is necessary for cocaine-associated memory formation (Supplementary Fig. 3). Our studies demonstrate that regulating AEA degradation through manipulation of FAAH governs cocaine-associated memory formation and that eCBs may represent a promising therapeutic target for cocaine addiction.

4.1. Disrupted AEA hydrolysis in the dDG during cocaine-associated memory formation

As retrograde signals, eCBs are released in both tonic and activity-dependent phasic modes [30–32]. 2-AG is a high-affinity agonist of CB1Rs, while AEA is a low-affinity agonist [11]. AEA is responsible for maintaining basal eCBs signalling, and 2-AG mediates strong and rapid signalling for inhibitory feedback via presynaptic CB1Rs [33]. These different actions are likely related to the fact that AEA is a partial

agonist at CB1Rs, while 2-AG acts as a full CBR1 agonist [34]. In our study, we showed that cocaine significantly increased the expression of the AEA in the dDG after cocaine CPP training. Our results indicated that AEA appears to play a more dominant role than 2-AG in regulating cocaine-associated memory formation, further supporting that different endogenous CB1R agonists exhibit different functions in the brain and have distinct effects. Regarding drug addiction, previous studies have reported that high levels of AEA may be involved in the rewarding effect of drugs and trigger various intracellular signalling cascades [35,36], although AEA alone was unable to impact quantal glutamate release at the central terminals [36]. In addition, increasing AEA signalling was shown to facilitate reinstatement induced by cocaine priming [37]. Our studies provide direct evidence of the degradation of AEA dysfunction in regulating CB1R activation in animal models of cocaine-associated memory, which is more reliant on AEA signalling than on 2-AG signalling.

4.2. CB1R signalling regulates hippocampal granule neuron dendritic spine structure during cocaine CPP training

eCBs have been reported to regulate mood, emotion and response to drugs through activation of CB1Rs [12,28]. Currently, regarding drug addiction, accumulated studies have focused on the role of CB1Rs in drug-induced relapse. For example, CB1R antagonists reduce excessive ethanol intake following periods of abstinence [38]. In contrast, administration of the CB1R agonist during alcohol abstinence increases post-abstinence elevations in alcohol consumption for up to 2 weeks after deprivation [39]. In addition, CB1R antagonism reduces the reinstatement of nicotine-seeking behaviour induced by either the presentation of discrete drug-paired cues [40] or exposure to environments previously paired with nicotine self-administration [41]. Thus, substantial evidence implicates CB1R signalling in drug-seeking behaviour for a variety of abused substances that differ substantially in their pharmacodynamic mechanisms, including cannabinoids, opioids, alcohol, nicotine and psychostimulants [4]. The hippocampus, a brain region strongly involved in cocaine-associated memory formation [16,17], presents a very high level of CB1Rs and mainly locate in cholecystokinin (CCK)-positive GABAergic interneurons [42,43]. Thus, the contribution of CB1Rs to memory formation associated with drug exposure is also likely.

The main finding of the present study is that CB1R signalling critically modulates cocaine-associated memory via activation of downstream molecules and alteration of dendritic spine structure. Our studies suggest that CB1R signalling is necessary for cocaine memory formation in an instrumental model of cocaine CPP, thereby expanding on the known involvement of CB1Rs in Pavlovian morphine, nicotine, and methamphetamine addiction [8–10]. In addition, previous reports have shown that CB1R signalling constitutes a potent activator of ERK and mTOR signalling [21,28]. Interestingly, cocaine-induced ERK and mTOR signalling activation, revealing CB1R activation of downstream molecules, is considered an emerging pathway for cocaine-associated memory formation. Collectively, the selective effects of CB1R antagonism on drug-associated memory formation are especially encouraging from the perspective of treating substance use disorders.

The structural and physiological properties of dendritic spine alterations are considered the primary mechanisms underlying cocaine-associated memory formation and are thought to be vital for the experience-dependent modifications in neural function that underlie behavioural flexibility [4,16]. To fully illustrate the morphological changes of dendritic spines that occur in the dDG following cocaine CPP training, we conducted high resolution imaging and 3D reconstruction to analysis the granule neurons dendritic spines. Results demonstrated that cocaine CPP mice showed an increase in spine density in dDG region of the hippocampus. In addition, this effect was not observed in the food CPP training and home cage cocaine injection. Thus, the alterations in spine density could be associated with the memory formation of an association between morphine and the environmental cues rather than an intrinsic effect of the drug by itself, especially cocaine given in the home cage has no effect on spine density. A possibility explanation is that the alterations in dendritic spines following the paired cocaine CPP could be due to the hippocampus neuron structural plasticity occurred specifically during the drug associated memory formation [44].

Previous studies have shown that CB1R signalling is involved in the ketamine-induced dendritic remodelling of spiny projection neurons in the dorsal lateral striatum [21]. However, little is known regarding the role of CB1R signalling in dendritic complexity in the dDG during cocaine-associated memory formation. In the present study, cocaine increased the dendritic complexity of granule neurons in the dDG, increasing the dendritic length and spine density of granule neurons. This observation is consistent with previous studies showing that cocaine enhances the remodelling of hippocampal neuron dendrite structure. Rimonabant is an inverse agonist of the CB1R, and the use of rimonabant has revealed the involvement of CB1Rs in operant nicotine and methamphetamine reward memory formation [9,10]. Furthermore, rimonabant attenuates nicotine relapse induced by associated environmental stimuli [45]. In the present study, intra-dDG infusion of rimonabant effectively inhibited granule neuron dendritic remodelling, further showing a critical role of CB1R signalling in cocaine-induced dendritic remodelling of granule neurons. Our findings indicated that CB1R signalling may selectively influence the structural and physiological properties of dendritic spines and further facilitate cocaine-associated memory formation.

4.3. Inhibition of FAAH in the dDG promotes cocaine-associated memory formation

The level of AEA is tightly regulated by the catabolic enzyme FAAH [46]. FAAH is highly expressed in brain regions implicated in reward and addiction and exerts widespread modulatory influences on molecular and behavioural responses to drugs of abuse [4,12]. Our studies revealed that cocaine resulted in a high concentration of AEA in the dDG and was associated with decreased FAAH levels and activity. FAAH inhibition promoted cocaine-associated memory formation. Our results revealed that FAAH is a key hydrolytic enzyme in mediating AEA production and plays an important role in cocaine-associated memory formation. Under normal physiological conditions, FAAH regulates AEA-induced stimulation of CB1Rs below the level associated with cocaine-associated memory formation. During cocaine-associated memory formation, cocaine significantly elevates the AEA level in the dDG by lowering FAAH expression; thus, excessive AEA triggers CB1R signalling and alters the dendritic spine structure of hippocampal granule neurons, contributing to cocaine-associated memory formation. Our results are consistent with previous studies reporting that pharmacological inhibition or genetic ablation of FAAH in rodents increases ethanol and nicotine preference as well as cocaine-induced psychomotor sensitization [12,47,48]. In addition, an FAAH polymorphism decreased brain levels of FAAH protein and increased levels of AEA [49] and enhanced the preference of adolescent mice for the cannabinoid $\triangle^9$-tetrahydrocannabinol (THC), which is persistently expressed into adulthood [50].

Previous research in nonhuman primates and rodents also demonstrates that pairing of contextual cues contributes to THC-associated

reward behaviour via CB1R-dependent dopamine activity [51,52]. FAAH inactivation of female mice contributes to cocaine-associated memory formation during adolescence [50]. Our results further elucidated the underlying neurobiological mechanism by which FAAH mediates AEA metabolism and AEA—CB1R signalling to induce downstream molecular activation and regulate dendritic structure remodelling during cocaine-associated memory formation. This evidence has translational value for assessing clinical symptoms of drug addiction and suggests a possible link between innate dysregulation of eCBs and drug addiction treatment.

In summary, this study highlights how FAAH changes AEA levels and AEA—CB1R signalling activation, causing increased vulnerability to cocaine addiction. However, chronic daily treatment with the CB1R inverse agonist rimonabant, while effective for smoking cessation, produces detrimental side effects in the form of neuropsychiatric disorders [53,54]. Rimonabant also shown to participate in pharmacological and behaviour effects independent of CB1 receptor activation as it is an inverse agonist of [55]. Thus, considering that CB1Rs are the main target of AEA in the present study, our results suggest that manipulating the metabolic production of AEA may be a promising strategy for inhibiting CB1R activation during cocaine-associated memory formation. The eCBs may serve as potential therapeutic targets for the treatment of cocaine addiction.

DATA AVAILABILITY

Data will be made available on request.

ACKNOWLEDGMENTS

This work was partially supported by the Postdoctoral Research fund of West China Hospital of Sichuan University (2021HXBH007), the Project funded by China Postdoctoral Science Foundation (2021M702373) and the National Natural Science Foundation of Sichuan Province (2022NSFSC1580).

CONFLICTS OF INTEREST

The authors declare no conflicts of interest.

APPENDIX A. SUPPLEMENTARY DATA

Supplementary data to this article can be found online at https://doi.org/10.1016/j.molmet.2022.101597.

REFERENCES

[1] Bender, B.N., Torregrossa, M.M., 2020. Molecular and circuit mechanisms regulating cocaine memory. Cellular and Molecular Life Sciences 77(19): 3745—3768.

[2] Crombag, H.S., Bossert, J.M., Koya, E., Shaham, Y., 2008. Review. Context-induced relapse to drug seeking: a review. Philosophical Transactions of the Royal Society of London B Biological Sciences 363(1507):3233—3243.

[3] Stringfield, S.J., Higginbotham, J.A., Wang, R., Berger, A.L., McLaughlin, R.J., Fuchs, R.A., 2017. Role of glucocorticoid receptor-mediated mechanisms in cocaine memory enhancement. Neuropharmacology 123:349—358.

[4] Sidhpura, N., Parsons, L.H., 2011. Endocannabinoid-mediated synaptic plasticity and addiction-related behavior. Neuropharmacology 61(7):1070—1087.

[5] Stern, C.A.J., de Carvalho, C.R., Bertoglio, L.J., Takahashi, R.N., 2018. Effects of cannabinoid drugs on Aversive or rewarding drug-associated memory extinction and reconsolidation. Neuroscience 370:62—80.

[6] Higginbotham, J.A., Wang, R., Richardson, B.D., Shiina, H., Tan, S.M., Presker, M.A., et al., 2021. CB1 receptor signaling modulates Amygdalar plasticity during context-cocaine memory reconsolidation to promote subsequent cocaine seeking. Journal of Neuroscience 41(4):613—629.

[7] He, X.H., Jordan, C.J., Vemuri, K., Bi, G.H., Zhan, J., Gardner, E.L., et al., 2019. Cannabinoid CB1 receptor neutral antagonist AM4113 inhibits heroin self-administration without depressive side effects in rats. Acta Pharmacologica Sinica 40(3):365—373.

[8] De Carvalho, C.R., Pamplona, F.A., Cruz, J.S., Takahashi, R.N., 2014. Endocannabinoids underlie reconsolidation of hedonic memories in Wistar rats. Psychopharmacology 231(7):1417—1425.

[9] Yu, L.L., Wang, X.Y., Zhao, M., Liu, Y., Li, Y.Q., Li, F.Q., et al., 2009. Effects of cannabinoid CB1 receptor antagonist rimonabant in consolidation and reconsolidation of methamphetamine reward memory in mice. Psychopharmacology 204(2):203—211.

[10] Fang, Q., Li, F.Q., Li, Y.Q., Xue, Y.X., He, Y.Y., Liu, J.F., et al., 2011. Cannabinoid CB1 receptor antagonist rimonabant disrupts nicotine reward-associated memory in rats. Pharmacology Biochemistry and Behavior 99(4):738—742.

[11] Pertwee, R.G., 2015. Endocannabinoids and their pharmacological actions. Handbook of Experimental Pharmacology 231:1—37.

[12] Parsons, L.H., Hurd, Y.L., 2015. Endocannabinoid signalling in reward and addiction. Nature Reviews Neuroscience 16(10):579—594.

[13] Sloan, M.E., Gowin, J.L., Ramchandani, V.A., Hurd, Y.L., Le Foll, B., 2017. The endocannabinoid system as a target for addiction treatment: trials and tribulations. Neuropharmacology 124:73—83.

[14] Xi, Z.X., Gilbert, J.G., Peng, X.Q., Pak, A.C., Li, X., Gardner, E.L., 2006. Cannabinoid CB1 receptor antagonist AM251 inhibits cocaine-primed relapse in rats: role of glutamate in the nucleus accumbens. Journal of Neuroscience 26(33):8531—8536.

[15] Fattore, L., Martellotta, M., Cossu, G., Mascia, M., Fratta, W.J.B., 1999. CB1 cannabinoid receptor agonist WIN 55,212-2 decreases intravenous cocaine self-administration in rats. Behavioural Brain Research 104:141—146.

[16] Li, H., Xu, W., Wang, D., Wang, L., Fang, Q., Wan, X., et al., 2021. 4R tau modulates cocaine-associated memory through Adult dorsal hippocampal neurogenesis. Journal of Neuroscience 41(31):6753—6774.

[17] Li, H., Zhou, X., Chen, R., Xiao, Y., Zhou, T., 2022. The src-kinase Fyn is required for cocaine-associated memory through regulation of tau. Frontiers in Pharmacology 13.

[18] Zheng, K., Hu, F., Zhou, Y., Zhang, J., Zheng, J., Lai, C., et al., 2021. miR-135a-5p mediates memory and synaptic impairments via the Rock2/Adducin1 signaling pathway in a mouse model of Alzheimer's disease. Nature Communications 12(1):1903.

[19] Scarante, F.F., Vila-Verde, C., Detoni, V.L., Ferreira-Junior, N.C., Guimaraes, F.S., Campos, A.C., 2017. Cannabinoid modulation of the stressed Hippocampus. Frontiers in Molecular Neuroscience 10:411.

[20] Kano, M., Ohno-Shosaku, T., Hashimotodani, Y., Uchigashima, M., Watanabe, M., 2009. Endocannabinoid-mediated control of synaptic transmission. Physiological Reviews 89(1):309—380.

[21] Xu, W., Li, H., Wang, L., Zhang, J., Liu, C., Wan, X., et al., 2020. Endocannabinoid signaling regulates the reinforcing and psychostimulant effects of ketamine in mice. Nature Communications 11(1):5962.

[22] Albrechet-Souza, L., Nastase, A.S., Hill, M.N., Gilpin, N.W., 2021. Amygdalar endocannabinoids are affected by predator odor stress in a sex-specific manner and modulate acoustic startle reactivity in female rats. Neurobiol Stress 15:100387.

[23] Luo, W., Mizuno, H., Iwata, R., Nakazawa, S., Yasuda, K., Itohara, S., et al., 2016. Supernova: a versatile vector system for single-cell labeling and gene function studies in vivo. Scientific Reports 6:35747.

[24] Sanchis-Segura, C., Spanagel, R.J.A.b., 2006. Behavioural assessment of drug reinforcement and addictive features in rodents: an overview. Addiction Biology 11(1):2—38.

[25] Bardo, M., Bevins, R.J.P., 2000. Conditioned place preference: what does it add to our preclinical understanding of drug reward? Psychopharmacology 153(1):31—43.
[26] Spanagel, R., 2020. Cannabinoids and the endocannabinoid system in reward processing and addiction: from mechanisms to interventions. Dialogues in Clinical Neuroscience 22(3):241—250.
[27] Jia, W., Kawahata, I., Cheng, A., Fukunaga, K., 2021. The role of CaMKII and ERK signaling in addiction. International Journal of Molecular Sciences 22(6).
[28] Chevalier, G., Siopi, E., Guenin-Mace, L., Pascal, M., Laval, T., Rifflet, A., et al., 2020. Effect of gut microbiota on depressive-like behaviors in mice is mediated by the endocannabinoid system. Nature Communications 11(1):6363.
[29] Meyer, H.C., Lee, F.S., Gee, D.G., 2018. The role of the endocannabinoid system and genetic variation in adolescent brain development. Neuropsychopharmacology 43(1):21—33.
[30] Ramikie, T.S., Nyilas, R., Bluett, R.J., Gamble-George, J.C., Hartley, N.D., Mackie, K., et al., 2014. Multiple mechanistically distinct modes of endocannabinoid mobilization at central amygdala glutamatergic synapses. Neuron 81(5):1111—1125.
[31] Baldi, R., Ghosh, D., Grueter, B.A., Patel, S., 2016. Electrophysiological measurement of cannabinoid-mediated synaptic modulation in Acute mouse brain slices. Current Protocols in Neuroscience 75:6 29 21, 26 29 19.
[32] Lee, S.H., Ledri, M., Toth, B., Marchionni, I., Henstridge, C.M., Dudok, B., et al., 2015. Multiple forms of endocannabinoid and endovanilloid signaling regulate the tonic control of GABA release. Journal of Neuroscience 35(27): 10039—10057.
[33] Mateo, Y., Johnson, K.A., Covey, D.P., Atwood, B.K., Wang, H.L., Zhang, S., et al., 2017. Endocannabinoid actions on cortical terminals orchestrate local modulation of dopamine release in the nucleus accumbens. Neuron 96(5): 1112—1126 e1115.
[34] Sugiura, T., Kishimoto, S., Oka, S., Gokoh, M., 2006. Biochemistry, pharmacology and physiology of 2-arachidonoylglycerol, an endogenous cannabinoid receptor ligand. Progress in Lipid Research 45(5):405—446.
[35] Zhang, L.-Y., Zhou, Y.-Q., Yu, Z.-P., Zhang, X.-Q., Shi, J., Shen, H.-W., 2021. Restoring glutamate homeostasis in the nucleus accumbens via endocannabinoid-mimetic drug prevents relapse to cocaine seeking behavior in rats. Neuropsychopharmacology.
[36] Fenwick, A.J., Fowler, D.K., Wu, S.W., Shaffer, F.J., Lindberg, J.E.M., Kinch, D.C., et al., 2017. Direct anandamide activation of TRPV1 produces divergent calcium and current responses. Frontiers in Molecular Neuroscience 10:200.
[37] You, I.J., Hong, S.I., Ma, S.X., Nguyen, T.L., Kwon, S.H., Lee, S.Y., et al., 2019. Transient receptor potential vanilloid 1 mediates cocaine reinstatement via the D1 dopamine receptor in the nucleus accumbens. Journal of Psychopharmacology 33(12):1491—1500.
[38] Gessa, G.L., Serra, S., Vacca, G., Carai, M.A., Colombo, G., 2005. Suppressing effect of the cannabinoid CB1 receptor antagonist, SR147778, on alcohol intake and motivational properties of alcohol in alcohol-preferring sP rats. Alcohol and Alcoholism 40(1):46—53.
[39] Alen, F., Moreno-Sanz, G., Isabel de Tena, A., Brooks, R.D., Lopez-Jimenez, A., Navarro, M., et al., 2008. Pharmacological activation of CB1 and D2 receptors in rats: predominant role of CB1 in the increase of alcohol relapse. European Journal of Neuroscience 27(12):3292—3298.
[40] De Vries, T.J., de Vries, W., Janssen, M.C., Schoffelmeer, A.N., 2005. Suppression of conditioned nicotine and sucrose seeking by the cannabinoid-1 receptor antagonist SR141716A. Behavioural Brain Research 161(1):164—168.
[41] Diergaarde, L., de Vries, W., Raaso, H., Schoffelmeer, A.N., De Vries, T.J., 2008. Contextual renewal of nicotine seeking in rats and its suppression by the cannabinoid-1 receptor antagonist Rimonabant (SR141716A). Neuropharmacology 55(5):712—716.
[42] Tsou, K., Brown, S., Sañudo-Peña, M., Mackie, K., Walker, J.J.N., 1998. Immunohistochemical distribution of cannabinoid CB1 receptors in the rat central nervous system. Neuroscience 83(2):393—411.
[43] Katona, I., Sperlágh, B., Sík, A., Käfalvi, A., Vizi, E., Mackie, K., et al., 1999. Presynaptically located CB1 cannabinoid receptors regulate GABA release from axon terminals of specific hippocampal interneurons. Journal of Neuroscience 19(11):4544—4558.
[44] Fakira, A.K., Massaly, N., Cohensedgh, O., Berman, A., Moron, J.A., 2016. Morphine-associated contextual cues induce structural plasticity in hippocampal CA1 pyramidal neurons. Neuropsychopharmacology 41(11):2668—2678.
[45] Cohen, C., Perrault, G., Griebel, G., Soubrie, P., 2005. Nicotine-associated cues maintain nicotine-seeking behavior in rats several weeks after nicotine withdrawal: reversal by the cannabinoid (CB1) receptor antagonist, rimonabant (SR141716). Neuropsychopharmacology 30(1):145—155.
[46] Hillard, C.J., 2015. The endocannabinoid signaling system in the CNS: a primer. International Review of Neurobiology 125:1—47.
[47] Solinas, M., Yasar, S., Goldberg, S.R., 2007. Endocannabinoid system involvement in brain reward processes related to drug abuse. Pharmacological Research 56(5):393—405.
[48] Zhou, Y., Huang, T., Lee, F., Kreek, M.J., 2016. Involvement of endocannabinoids in alcohol "Binge" drinking: studies of mice with human fatty acid amide hydrolase genetic variation and after CB1 receptor antagonists. Alcoholism: Clinical and Experimental Research 40(3):467—473.
[49] Dincheva, I., Drysdale, A.T., Hartley, C.A., Johnson, D.C., Jing, D., King, E.C., et al., 2015. FAAH genetic variation enhances fronto-amygdala function in mouse and human. Nature Communications 6:6395.
[50] Burgdorf, C., Jing, D., Yang, R., Huang, C., Hill, M., Mackie, K., et al., 2020. Endocannabinoid genetic variation enhances vulnerability to THC reward in adolescent female mice. Science Advances 6(7):eaay1502.
[51] Panlilio, L.V., Justinova, Z., 2018. Preclinical studies of cannabinoid reward, treatments for cannabis use disorder, and addiction-related effects of cannabinoid exposure. Neuropsychopharmacology 43(1):116—141.
[52] Oleson, E.B., Cheer, J.F., 2012. A brain on cannabinoids: the role of dopamine release in reward seeking. Cold Spring Harbor Perspectives in Medicine 2(8).
[53] Sun, Y., Chen, J., 2012. Rimonabant, gastrointestinal motility and obesity. Current Neuropharmacology 10(3):212—218.
[54] Moreira, F., Crippa, J., 2009. The psychiatric side-effects of rimonabant. Revista Brasileira de Psiquiatria 31(2):145—153.
[55] Hu, S.S., 2016. Involvement of TRPV1 in the olfactory Bulb in rimonabant-induced olfactory discrimination deficit. The Chinese Journal of Physiology 59(1):21—32.

